Quantification of myocardial interstitial fibrosis and extracellular volume for the detection of cardiac allograft vasculopathy

van Heeswijk, Ruud B; Bastiaansen, Jessica A M; Iglesias, Juan Fernando; Degrauwe, Sophie; Rotman, Samuel; Barras, Jean-Luc; Regamey, Julien; Lauriers, Nathalie; Tozzi, Piergiorgio; Yerly, Jérôme; Ginami, Giulia; Stuber, Matthias; Hullin, Roger

How to cite

VAN HEESWIJK, Ruud B et al. Quantification of myocardial interstitial fibrosis and extracellular volume for the detection of cardiac allograft vasculopathy. In: The international journal of cardiovascular imaging, 2020, vol. 36, n° 3, p. 533–542. doi: 10.1007/s10554-019-01733-3

This publication URL: https://archive-ouverte.unige.ch//unige:163364
Publication DOI: 10.1007/s10554-019-01733-3

Title: Quantification of myocardial interstitial fibrosis and extracellular volume for the detection of cardiac allograft vasculopathy
Authors: Ruud B. van Heeswijk, Jessica A.M. Bastiaansen, Juan F. Iglesias, Sophie Degrauwe, Samuel Rotman Jean-Luc Barras, Julien Regamey, Nathalie Lauriers, Piergiorgio Tozzi, Jérôme Yerly, Giulia Ginami, Matthias Stuber, Roger Hullin
Journal: The international journal of cardiovascular imaging
Year: 2019
Volume: 3
Issue: 34
Pages: 73-97
DOI: 10.1007/s10554-019-01733-3

Authors' names: Ruud B. van Heeswijk, PhD[a,d]*, Jessica A.M. Bastiaansen, PhD[a], Juan F. Iglesias, MD[b,e], Sophie Degrauwe, MD[b,e], Samuel Rotman, MD[c], Jean-Luc Barras, MD[c], Julien Regamey, MD[b], Nathalie Lauriers, RN[b], Piergiorgio Tozzi, MD[b], Jérôme Yerly, PhD[a,d], Giulia Ginami, PhD[a,f], Matthias Stuber, PhD[a,d], Roger Hullin, MD[b]

Title: Quantification of myocardial interstitial fibrosis and extracellular volume for the detection of cardiac allograft vasculopathy

Affiliations: (a) Radiology, (b) Cardiology and Cardiac Surgery, (c) Clinical Pathology, Lausanne University Hospital (CHUV) and University of Lausanne (UNIL), Lausanne, Switzerland; (d) Center for Biomedical Imaging, Lausanne; (e) Cardiology, University Hospital of Geneva (HUG), Switzerland; (f) Siemens Healthcare GmbH, Siemens AG, Erlangen, Germany

***Corresponding author**: Ruud B. van Heeswijk - ruud.mri@gmail.com, +41-213147535

ORCIDs: Ruud B. van Heeswijk (0000-0001-5028-4521), Jessica A.M. Bastiaansen (0000-0002-5485-1308), Samuel Rotman (0000-0002-2508-3725), Jérôme Yerly (0000-0003-4347-8613), Giulia Ginami (0000-0003-4669-0572), Matthias Stuber (0000-0001-9843-2028)

Acknowledgements: This work was supported by grants from the Swiss Heart Foundation to RH, JAMB and RBvH, and from the Swiss National Science Foundation to RBvH (PZ00P3_154719 and 32003B_182615), RH (320030_147121), JAMB (PZ00P3_167871) and MS (320030_143923, 326030_150828, and 320030_173129). MS received non-monetary research support from Siemens Healthineers.

Abstract

Purpose

In search of a non-invasive alternative detection of early-stage cardiac allograft vasculopathy (CAV), in the preliminary study we tested the hypothesis that interstitial fibrosis quantified with cardiac magnetic resonance (CMR) can serve as a biomarker for the detection of CAV.

Methods

Late-stage CAV was detected with routine X-ray coronary angiography (XRCA), while a coronary intima-media thickness ratio (IMTR)>1 on optical coherence tomography (OCT) was used to detect early-stage CAV. Interstitial fibrosis was quantified in the endomyocardial biopsy (EMB) and indirectly with CMR as the T1 relaxation time and extracellular volume (ECV). CMR was performed within 48h of a single invasive procedure with XRCA, OCT, and EMB procurement in stable HTx recipients (n=27; age 54±13y, 5.4±3.7y posttransplant).

Results

XRCA-CAV and IMTR>1 were present in 15% and 75% of study patients, respectively. The T_1 relaxation times and ECV were increased in patients with XRCA-CAV (p=0.03 each), while IMTR and EMB interstitial fibrosis were not significantly different (both P>0.05). ECV (ρ=0.46, P=0.02) and IMTR (ρ=0.58; P=0.01) correlated with the histological quantity of interstitial fibrosis, while the T_1 relaxation time (P=0.06) did not.

Conclusions

The correlation of the IMTR with the EMB interstitial fibrosis tentatively validates the hypothesis that interstitial fibrosis may serve as an early indicator of CAV. Moreover, the significant association of CMR-based ECV with the magnitude of interstitial fibrosis in the biopsy suggests ECV as a potential biomarker

for interstitial fibrosis due to early-stage CAV. The measurement of ECV may therefore have a role for non-invasive detection and follow-up of early-stage CAV.

Keywords

Cardiac allograft vasculopathy, interstitial fibrosis, cardiovascular magnetic resonance, extracellular volume, optical coherence tomography, heart transplantation

Introduction

Heart transplantation (HTx) remains the definitive treatment for eligible patients with end-stage heart failure. Survival after heart transplantation has substantially increased during the last two decades due to the significant decrease of all-cause mortality primarily within the first 12 months. However, the mid- and long-term survival after HTx has not substantially improved [1].

Cardiac allograft vasculopathy (CAV) is still among the leading causes of mid-term and late post-transplant mortality [1], despite significant effort to increase comprehension of the complex interplay of various contributing factors [2], CAV is characterized by diffuse intimal hyperplasia that affects the coronary circulation in a longitudinal and concentric arteriovascular pattern [3]. Invasive X-ray based coronary angiography (XRCA) remains the routine for CAV detection but is primarily sensitive to luminal pathology, which is a characteristic of late-stage CAV [4]. High-resolution optical coherence tomography (OCT) enables the visualization of the inner layers of the coronary artery vessel wall and has recently been used for the detection of intimal hyperplasia, which has been shown to occur already early after HTx when luminopathologic changes characteristics of CAV are not present [5,6]. The spatial resolution of OCT (10-20 µm) is ten-fold higher than that of intravascular ultrasound (IVUS, 100-150 µm), and while the penetration depth is lower, it thus allows for an accurate high-resolution visualisation of the tunica intima and media [6]. However, OCT-based imaging of the coronary vascular wall is not extensively applied for technical and financial reasons as well as its need for extra contrast medium, which precludes the standard application of this technique in HTx recipients with more advanced kidney disease [7]. All the same, detection of early-stage CAV remains essential since immunosuppression with mTOR (mammalian target of rapamycin) inhibition has the potential to slow or even inhibit CAV progression if introduced before the advent of irreversible damage of the coronary artery vessel wall [8].

Histological studies suggest that CAV starts with endothelial injury [2,9], followed by capillary rarefication [10,11] and impaired adaptation of the myocardial blood flow to exercise-induced myocardial oxygen

demand (Figure 1). Subsequent diffuse myocardial hypoxia has been shown to result in an increase of the magnitude of interstitial fibrosis [12,13], which led us to hypothesize that myocardial interstitial fibrosis could be not only a biomarker for late-stage CAV, but for early-stage CAV as well. Myocardial fibrosis can be quantified by gold-standard automated colour segmentation of histological images obtained from endomyocardial biopsy (EMB) [14], and has been shown to strongly correlate with the myocardial longitudinal (T_1) relaxation time and extracellular volume (ECV) that can be non-invasively mapped with cardiovascular magnetic resonance (CMR) [15,16]. These two quantitative CMR measures differ in that native (i.e. pre-contrast-agent) T_1 mapping is sensitive to changes in many components of the myocardium, which for example also includes changes caused by oedema, which makes it less specific in many cases [16]. The ECV, however, exploits the extracellular nature of contrast agents and is a measure of the non-cellular space that is mostly occupied by the extracellular matrix. Since the extracellular matrix is largely composed of collagen fibres, ECV correlates with the myocardial collagen volume fraction as already shown across different entities of human cardiac pathology [17,18]. However, it should also be noted that ECV cannot be measured in all HTx recipients because of the potentially serious secondary effects of gadolinium-based contrast agents in those with more advanced renal insufficiency.

Therefore, as a proof of the concept that the non-invasive measurement of interstitial fibrosis could serve as an alternative to invasive screening of CAV, the aim of this study was to test the hypothesis that the amount of myocardial interstitial fibrosis as quantified with CMR can serve as a biomarker for the detection of CAV.

Methods

Study population

The local ethics committee approved the study; all participants provided written informed consent (protocol CER Vaud 2016-00635). All experiments were performed in accordance with relevant guidelines and regulations. Stable cardiac allograft transplant patients (n=27, mean age: 54±13 years) (Table 1) at least 6

months after surgery were included (average post-transplant time: 5.4±3.7 years, range 1-17 years) in order to investigate CAV from early onset to more advanced stages. HTx recipients without complete explantation of cardiovascular implantable electronic devices or with residual leads were excluded. HTx recipients with an estimated glomerular filtration rate (GFR) <30 ml/min/1.73 m^2, claustrophobia, or acute cellular rejection in the preceding EMB were not included. Donor hearts were always free of segmental dyskinesia on echocardiography. Donor coronary angiograms obtained in ≥50 years-old donors were free of significant luminal pathology. Induction therapy in the immediate postoperative phase was started with thymoglobulin in 37% of patients and with basiliximab in 63% of study participants. Immunosuppressive maintenance therapy was adapted to the individual patient within the limits of the site-specific protocol [4]. XRCA, OCT and EMB procurement were performed within one single per-protocol intervention; CMR was always performed within 48 hours of this intervention. All study participants were treated with valganciclovir for at least 3 months in the immediate phase after HTx; cytomegalovirus (CMV)-negative HTx recipients with CMV-positive donor cardiac allograft received 6 months of treatment.

Coronary X-ray angiography

Routine XRCA was performed on standard equipment (Allura, Philips, Amsterdam, The Netherlands) using a 6F guiding catheter via right radial or right femoral artery access. The coronary arteries were imaged after administration of intracoronary nitro-glycerine (50 μg) into the right coronary artery (RCA) or left main coronary artery. At least two orthogonal projections of each coronary artery were acquired. Two interventional cardiologists (J.F.I. and S.D.) independently graded the severity of CAV (hereafter called XRCA-CAV) with a scale ranging from 0 (=not significant) to 3 (=severe) on the basis of luminographic pathology [4], which remains the clinical reference standard even though it can only be used to detect late-stage CAV. In cases of differences in CAV grading, a consensus was sought after joint reinvestigation.

Optical coherence tomography

OCT was performed using a Dragonfly Optis Imaging catheter system (St. Jude Medical, St. Paul, Minnesota, USA) in 24/27 patients. The catheter was placed either into the middle segment of the RCA or

the left anterior descending artery. After intracoronary administration of 50 µg nitro-glycerine, OCT imaging was performed by automated pullback over 54 mm at a speed of 20 mm/s, a radial resolution of 20 µm, and a frame density of 10 frames/mm. Quantitative cross-sectional OCT analysis was performed off-line using a dedicated OCT workstation (Ilumien Optis Offline Review Workstation, St. Jude Medical, St. Paul, Minnesota, USA). All cross-sectional images were initially reviewed for quality. Frames were excluded when a side branch was present in >45° of the cross section, in the case of inadequate image quality due to residual blood, artefact or reverberation, or if segments contained atherosclerotic plaque. The layers were analysed according to OCT consensus standard definitions [19]. The lumen, intima and media layers were traced manually every 5±2 frames starting at 35 mm from the vessel ostium. Vessel layer assessment included measurements of lumen area, intima layer area and media layer area obtained by averaging the lumen-intima, intima-media and media-adventitia interface contours for the entire analysed segment. The intima-media thickness ratio (IMTR) was calculated by dividing the average area of each layer over the 35 mm of the analysed vessel. An IMTR >1 was considered pathologic [6], and will be referred to as OCT-CAV.

Histology of the endomyocardial biopsy

The quantification of interstitial fibrosis in the individual study patient was based on Van Gieson's staining [14] of 3 separate EMB specimens. Slides were scanned with a NanoZoomer S60 (Hamamatsu Photonics, Hamamatsu, Japan) with a spatial resolution of 2.2 pixels/µm (i.e. 454 nm). The percentage of fibrosis was then automatically quantified by colour segmentation with SlidePath (Leica Biosystems, Wetzlar, Germany). Samples that included scar tissues from previous biopsy sites were excluded to avoid confounding the quantification of pathological interstitial fibrosis with scar fibrosis.

Cardiovascular magnetic resonance

Myocardial segmented k-space T_1 mapping (breath-held MOLLI [20], slice thickness 8mm, RF excitation angle 35°, echo time 1.12ms, repetition time 3.2ms, matrix size 256×144 interpolated to 256×218,

interpolated pixel size 1.9×1.9mm^2, parallel imaging (GRAPPA) factor 2, pixel bandwidth 1085 Hz/pixel) was used to assess 2 short-axis slices (1 midventricular and 1 basal) at a magnetic field strength of 3T (Magnetom Prisma, Siemens Healthcare, Erlangen, Germany) with a 32-element RF coil for signal reception. Maps were acquired before and 19-27 min after gadolinium contrast agent injection (Gadovist, 0.1 ml/kg) in the 48h following XRCA. A 3(3)5 MOLLI scheme was used pre-contrast, while a 4(1)3(1)2 scheme was used post-contrast. Pre- and post- contrast T_1 maps were generated in Matlab (The Mathworks, Natick, Massachusetts, USA), after which the entire myocardium was segmented, and both the native T_1 and ECV of the entire segmented myocardium of both slices were computed. Cine functional imaging and late gadolinium enhancement were not performed due to time constraints. Haematocrit (Hct) was assessed as part of the routine blood workup on the same day as the EMB.

Statistical analyses

An unpaired two-tailed Student's t-test was used to establish whether the presence of XRCA-CAV is linked to differences in IMTR, EMB-based quantification of interstitial fibrosis, T_1 relaxation time, or ECV. A Pearson correlation was calculated to ascertain whether there is a link between the IMTR or fibrosis on the one hand, and the T_1 or ECV values on the other hand. $P<0.05$ was considered significant, and Bonferroni correction was used to compensate for multiple comparisons. Receiver-operator curves (ROC) were generated for all techniques to detect XRCA-CAV>0 and IMTR>1, and the area under the curve (AUC) was calculated. All calculations were performed in Matlab and Prism (Graphpad, La Jolla, California, USA).

Results

No medical complications related to the procedures occurred in any of the patients. Clinical characteristics of the study participants are summarized in Table 1. First, the measurements of vascular characteristics (XRCA and OCT) and myocardial characteristics (histology and CMR) are reported by themselves. This is followed by the observed differences between grouped XRCA-CAV-positive and -negative patients.

Finally, the correlations between the EMB fibrosis and the other modalities as well as the correlations between the IMTR and the other modalities are presented.

Vascular characteristics

XRCA was successfully completed in all patients (Table 2, Supplementary Table 1). Four study participants presented XRCA-CAV (15%) with an average grade of 1.5±1.0 (Figure 2A,B). Non-significant focal atherosclerotic lesions were visualized on XRCA in 11/27 patients (41%; 3 single-vessel, 3 two-vessels, 5 three-vessel disease).

High-quality OCT images were obtained in 20/27 patients (74%, Figure 2C-F); insufficient image quality was caused by incomplete blood washout during data acquisition (n=4 patients), diffuse atherosclerosis (n=2 patients), and technical complications (n=1). Most OCT data were acquired in the right coronary artery (n=18 patients); 2 datasets were obtained in the left anterior descending coronary artery because of anticipated incomplete blood washout in the dominant RCA. Pathologic IMTR was present in 15/20 patients (75%); the average IMTR was 1.56±0.63 (range 0.68-2.71). All patients with XRCA-CAV had IMTR>1; their average IMTR was 2.01±0.81.

Myocardial characteristics

Histological analysis of the EMB was performed in 25/27 patients (93%, Figure 3A,B, Table 2); 1 EMB was scar tissue only, and 1 procurement was not performed due to technical difficulties. Colour segmentation demonstrated a wide range of interstitial fibrosis (average 29±20%, range 5-78%).

CMR resulted in high-quality pre- and post-contrast T_1 maps in all patients (Figure 3C-F). The myocardium appeared homogeneous on all native and post-contrast maps, i.e. no focal or patchy T_1 elevation was observed, which indicates the absence of magnetic field inhomogeneities, artefacts, and focal disease. The average myocardial T_1 relaxation time was 1256±49 ms (range 1169-1382 ms) pre-gadolinium, while it amounted to 623±61 ms (range 544-852 ms) post-gadolinium. This resulted in an average myocardial ECV of 31.9±4.8% (range 26.5-49.8%).

Associations with XRCA-based detection of CAV

Interstitial fibrosis quantified by colour segmentation of the EMB as well as IMTR were not significantly different between groups with or without XRCA-CAV (P=0.11 and P=0.25, respectively), although both were numerically higher in patients with XRCA-CAV (Figure 4A,B). By contrast, T_1 values and ECV were both significantly higher in recipients with XRCA-CAV (P=0.03 both, Figure 4C,D). The ROC analysis for the detection of XRCA-CAV>0 showed a similar moderate AUC for all techniques: 0.74 (P=0.14) for IMTR, 0.71 (P=0.14) for histology, 0.73 (P=0.15) for the T_1 relaxation time, and 0.75 (P=0.12) for the ECV.

Correlations with interstitial fibrosis and intimal thickening

The magnitude of histological interstitial fibrosis correlated by trend with the native T_1 relaxation time (ρ=0.37; P=0.06) and significantly with ECV (ρ=0.46; P=0.02, Figure 5A,B) in accordance with previous studies reporting on other human cardiac pathologies [21,22]. IMTR was significantly correlated with the amount of histological interstitial fibrosis (ρ=0.58; P=0.01, Figure 6A), but was associated with neither the T_1 relaxation time nor with the ECV (Figure 6B,C). The ROC analysis for the detection of OCT-CAV (i.e. IMTR>1) agreed with these observations, and resulted in low AUC values for the XRCA-CAV score (AUC=0.67, P=0.26), T_1 relaxation time (AUC=0.55, P=0.63), and ECV (AUC=0.68, P=0.27), while the histology had a moderate AUC of 0.79 (P=0.07).

Discussion

In this study we used five different measurements of pathologic features associated with cardiac allograft vasculopathy (CAV) in order to assess whether interstitial fibrosis as quantified with CMR could serve as a surrogate marker for CAV. XRCA was used for characterization of late-stage CAV with luminal pathology, while OCT was applied for detection of intramural disease that is representative of early-stage CAV. The amount of interstitial fibrosis, already known as a primary non-vascular sequela of CAV in its later stages [23,24], was quantified both histologically in the EMB and indirectly by CMR-based mapping of the T_1

relaxation time and ECV - both recently established techniques in clinical routine [16]. This study confirms 1) the hypothesis that the amount of interstitial fibrosis in the biopsy of the cardiac allograft increases with the intima-media thickness ratio (IMTR), which is the most sensitive marker for early-stage CAV [25], and 2) that the measurement of ECV correlates with the magnitude of interstitial fibrosis in the biopsy.

CAV remains a major limitation for long-term success after cardiac transplantation. However, recent evidence suggests that conversion of immunosuppression to the mammalian target of rapamycin (mTOR) attenuates disease progression in particular in cases with early-stage CAV [23,24]. Recently, OCT has been used to show that the intima area increases by 20% within the first year after HTx while there was an overall 2% decrease of the coronary lumen [25]. These results indicate that intimal pathology already occurs early after HTx, and that OCT is highly suited for diagnosis and follow-up of early-stage CAV. OCT measures in the present study showed that a pathological IMTR of >1 was present in 75% of all study participants, while luminal (late-stage) pathology associated with CAV was present in only 15% of all study participants. The high prevalence of pathologic IMTR can explain why IMTR was not significantly different between HTx recipients with or without XRCA-CAV suggesting that intimal hyperplasia preceded the advent of intraluminal pathology in the majority of study participants [4]. In fact, every study participant with XRCA-CAV had a pathologic IMTR in the present study. These observations together with the widely different prevalence of intraluminal CAV pathology and pathologic IMTR provide further support to the idea that intima proliferation precedes luminal pathology [6,23,25] and that OCT is the most suited diagnostic means for detection of early-stage CAV.

However, OCT is an invasive, expensive, and technically demanding exam, which limits its broad application. We therefore investigated the interrelation of interstitial fibrosis with early-stage CAV. IMTR correlated strongly with the magnitude of interstitial fibrosis in the endomyocardial biopsy in the present study, indicating that early-stage CAV is already associated with an increase of cardiac allograft interstitial fibrosis. In fact, in another study it was found that the magnitude of interstitial fibrosis increased with time after heart transplantation, and that this progression was accompanied with an augmented expression of

biomarkers of hypoxia, the oxygen sensor prolyl hydroxylase 3, and the vascular endothelial growth factor [13]. The increase of myocardial fibrosis is thus most likely not exclusively limited to advanced vasculopathy as suggested earlier [26], but might occur already with early-stage CAV. This makes the detection of early-stage CAV even more essential, because the increase of myocardial fibrosis contributes to diastolic and systolic dysfunction of the cardiac allograft [27], which reduce the benefit of heart transplantation.

Native T_1 mapping and ECV measurement introduced novel quantitative metrics for the assessment of alteration of tissue composition after heart transplantation. Post-contrast T_1 mapping, which can be seen as a quantitative version of the widely used late gadolinium enhancement (LGE) imaging, did not reveal focal signal elevation in the present study. This indicates the absence of scar tissue, which can result either from more severe acute rejection or from advanced CAV with occlusion of peripheral coronary segments. ECV correlated well with the amount of interstitial fibrosis in the biopsy, which is in accordance with findings in studies of other cardiac pathologies [17,18]. Although significant, the correlation coefficients are still relatively low, which might be attributed to the small sample size and the heterogeneous patient population. We did not observe a correlation between the IMTR and ECV, while both correlated with histological interstitial fibrosis. At this point it remains to be determined whether this observation relates to the number of study participants or the largely different spatial resolution and coverage of OCT and CMR. No local cohort of age-matched healthy volunteers was available to put the T_1 and ECV values obtained at 3T in a local context; this remains of interest for follow-up studies.

The main limitation of this pilot study is the small number of included patients, which can explain the low to modest areas under the curve (AUC) in the ROC analyses and the associated non-significant P-values. However, it should be noted that other studies in which OCT was applied for the detection of early-stage CAV included a similar number of study participants [6,25]. Larger patient numbers were only investigated after pilot studies [28,29], which is most likely related to the complexity and cost of OCT-based investigation.

In conclusion, the present pilot study tentatively confirms the hypothesis that CAV as established by pathologic IMTR in OCT is already associated with increase of histological interstitial fibrosis. Similar to other human cardiac pathology, ECV measurement and histological interstitial fibrosis correlated well in this study suggesting that a CMR-based ECV measurement provides an option for non-invasive detection of the magnitude of interstitial fibrosis in the cardiac allograft. These promising results need further investigation in a larger scale study, which should test both prediction of ECV for CAV and the reproducibility of this measure for follow-up in clinical routine.

Additional Information

Ethics approval and consent to participate

All procedures performed in studies involving human participants were in accordance with the ethical standards of the institutional and/or national research committee (Cantonal Ethics Committee for Research in the Canton of Vaud – CER-VD, protocol 2016-00635) and with the 1964 Helsinki declaration and its later amendments or comparable ethical standards. Written informed consent was obtained from all individual participants included in the study.

Availability of data and materials

The datasets used and analysed during the current study are available from the corresponding author on reasonable request.

Competing interests statement

The authors declare that they have no competing interests.

References

1. Lund LH, Khush KK, Cherikh WS, Goldfarb S, Kucheryavaya AY, Levvey BJ, Meiser B, Rossano JW, Chambers DC, Yusen RD, Stehlik J, International Society for H, Lung T (2017) The Registry of the International Society for Heart and Lung Transplantation: Thirty-fourth Adult Heart Transplantation Report-2017; Focus Theme: Allograft ischemic time. J Heart Lung Transplant 36 (10):1037-1046. doi:10.1016/j.healun.2017.07.019

2. Schmauss D, Weis M (2008) Cardiac allograft vasculopathy: recent developments. Circulation 117 (16):2131-2141. doi:10.1161/CIRCULATIONAHA.107.711911

3. Rahmani M, Cruz RP, Granville DJ, McManus BM (2006) Allograft vasculopathy versus atherosclerosis. Circ Res 99 (8):801-815. doi:10.1161/01.RES.0000246086.93555.f3

4. Mehra MR, Crespo-Leiro MG, Dipchand A, Ensminger SM, Hiemann NE, Kobashigawa JA, Madsen J, Parameshwar J, Starling RC, Uber PA (2010) International Society for Heart and Lung Transplantation working formulation of a standardized nomenclature for cardiac allograft vasculopathy-2010. J Heart Lung Transplant 29 (7):717-727. doi:10.1016/j.healun.2010.05.017

5. Yeung AC, Davis SF, Hauptman PJ, Kobashigawa JA, Miller LW, Valantine HA, Ventura HO, Wiedermann J, Wilensky R (1995) Incidence and progression of transplant coronary artery disease over 1 year: results of a multicenter trial with use of intravascular ultrasound. Multicenter Intravascular Ultrasound Transplant Study Group. J Heart Lung Transplant 14 (6 Pt 2):S215-220

6. Khandhar SJ, Yamamoto H, Teuteberg JJ, Shullo MA, Bezerra HG, Costa MA, Selzer F, Lee JS, Marroquin OC, McNamara DM, Mulukutla SR, Toma C (2013) Optical coherence tomography for characterization of cardiac allograft vasculopathy after heart transplantation (OCTCAV study). J Heart Lung Transplant 32 (6):596-602. doi:10.1016/j.healun.2013.02.005

7. Estep JD, Shah DJ, Nagueh SF, Mahmarian JJ, Torre-Amione G, Zoghbi WA (2009) The role of multimodality cardiac imaging in the transplanted heart. JACC Cardiovasc Imaging 2 (9):1126-1140. doi:10.1016/j.jcmg.2009.06.006

8. Gude E, Gullestad L, Andreassen AK (2017) Everolimus immunosuppression for renal protection, reduction of allograft vasculopathy and prevention of allograft rejection in de-novo heart transplant recipients: could we have it all? Current opinion in organ transplantation 22 (3):198-206. doi:10.1097/MOT.0000000000000409

9. Tan CD, Baldwin WM, 3rd, Rodriguez ER (2007) Update on cardiac transplantation pathology. Archives of pathology & laboratory medicine 131 (8):1169-1191. doi:10.1043/1543-2165(2007)131[1169:UOCTP]2.0.CO;2

10. Hiemann NE, Meyer R, Wellnhofer E, Klimek WJ, Bocksch W, Hetzer R (2001) Correlation of angiographic and immunohistochemical findings in graft vessel disease after heart transplantation. Transplant Proc 33 (1-2):1586-1590

11. Broyd CJ, Hernandez-Perez F, Segovia J, Echavarria-Pinto M, Quiros-Carretero A, Salas C, Gonzalo N, Jimenez-Quevedo P, Nombela-Franco L, Salinas P, Nunez-Gil I, Del Trigo M, Goicolea J, Alonso-Pulpon L, Fernandez-Ortiz A, Parker K, Hughes A, Mayet J, Davies J, Escaned J (2018) Identification of capillary rarefaction using intracoronary wave intensity analysis with resultant prognostic implications for cardiac allograft patients. Eur Heart J 39 (20):1807-1814. doi:10.1093/eurheartj/ehx732

12. Gyongyosi M, Winkler J, Ramos I, Do QT, Firat H, McDonald K, Gonzalez A, Thum T, Diez J, Jaisser F, Pizard A, Zannad F (2017) Myocardial fibrosis: biomedical research from bench to bedside. Eur J Heart Fail 19 (2):177-191. doi:10.1002/ejhf.696

13. Gramley F, Lorenzen J, Pezzella F, Kettering K, Himmrich E, Plumhans C, Koellensperger E, Munzel T (2009) Hypoxia and myocardial remodeling in human cardiac allografts: a time-course study. J Heart Lung Transplant 28 (11):1119-1126. doi:10.1016/j.healun.2009.05.038

14. Studeli R, Jung S, Mohacsi P, Perruchoud S, Castiglioni P, Wenaweser P, Heimbeck G, Feller M, Hullin R (2006) Diastolic dysfunction in human cardiac allografts is related with reduced SERCA2a gene expression. Am J Transplant 6 (4):775-782. doi:10.1111/j.1600-6143.2006.01241.x

15. Schelbert EB, Fonarow GC, Bonow RO, Butler J, Gheorghiade M (2014) Therapeutic targets in heart failure: refocusing on the myocardial interstitium. J Am Coll Cardiol 63 (21):2188-2198. doi:10.1016/j.jacc.2014.01.068

16. Messroghli DR, Moon JC, Ferreira VM, Grosse-Wortmann L, He T, Kellman P, Mascherbauer J, Nezafat R, Salerno M, Schelbert EB, Taylor AJ, Thompson R, Ugander M, van Heeswijk RB, Friedrich MG (2017) Clinical recommendations for cardiovascular magnetic resonance mapping of T1, T2, T2* and extracellular volume: A consensus statement by the Society for Cardiovascular Magnetic Resonance (SCMR) endorsed by the European Association for Cardiovascular Imaging (EACVI). J Cardiovasc Magn Reson 19 (1):75. doi:10.1186/s12968-017-0389-8

17. White SK, Sado DM, Fontana M, Banypersad SM, Maestrini V, Flett AS, Piechnik SK, Robson MD, Hausenloy DJ, Sheikh AM, Hawkins PN, Moon JC (2013) T1 mapping for myocardial extracellular volume measurement by CMR: bolus only versus primed infusion technique. JACC Cardiovasc Imaging 6 (9):955-962. doi:10.1016/j.jcmg.2013.01.011

18. Cui Y, Cao Y, Song J, Dong N, Kong X, Wang J, Yuan Y, Zhu X, Yan X, Greiser A, Shi H, Han P (2018) Association between myocardial extracellular volume and strain analysis through cardiovascular magnetic resonance with histological myocardial fibrosis in patients awaiting heart transplantation. J Cardiovasc Magn Reson 20 (1):25. doi:10.1186/s12968-018-0445-z

19. Tearney GJ, Regar E, Akasaka T, Adriaenssens T, Barlis P, Bezerra HG, Bouma B, Bruining N, Cho JM, Chowdhary S, Costa MA, de Silva R, Dijkstra J, Di Mario C, Dudek D, Falk E, Feldman MD, Fitzgerald P, Garcia-Garcia HM, Gonzalo N, Granada JF, Guagliumi G, Holm NR, Honda Y, Ikeno F, Kawasaki M, Kochman J, Koltowski L, Kubo T, Kume T, Kyono H, Lam CC, Lamouche G, Lee DP, Leon MB, Maehara A, Manfrini O, Mintz GS, Mizuno K, Morel MA, Nadkarni S, Okura H, Otake H, Pietrasik A, Prati F, Raber L, Radu MD, Rieber J, Riga M, Rollins A, Rosenberg M, Sirbu V, Serruys PW, Shimada K, Shinke T, Shite J, Siegel E, Sonoda S, Suter M, Takarada S, Tanaka A, Terashima M, Thim T, Uemura S, Ughi GJ, van Beusekom HM, van der Steen AF, van Es GA, van Soest G, Virmani R, Waxman S, Weissman NJ, Weisz G, International Working Group for Intravascular Optical Coherence Tomography (2012) Consensus

standards for acquisition, measurement, and reporting of intravascular optical coherence tomography studies: a report from the International Working Group for Intravascular Optical Coherence Tomography Standardization and Validation. J Am Coll Cardiol 59 (12):1058-1072. doi:10.1016/j.jacc.2011.09.079

20. Messroghli DR, Radjenovic A, Kozerke S, Higgins DM, Sivananthan MU, Ridgway JP (2004) Modified Look-Locker inversion recovery (MOLLI) for high-resolution T1 mapping of the heart. Magn Reson Med 52 (1):141-146. doi:10.1002/mrm.20110

21. Fontana M, White SK, Banypersad SM, Sado DM, Maestrini V, Flett AS, Piechnik SK, Neubauer S, Roberts N, Moon JC (2012) Comparison of T1 mapping techniques for ECV quantification. Histological validation and reproducibility of ShMOLLI versus multibreath-hold T1 quantification equilibrium contrast CMR. J Cardiovasc Magn Reson 14:88. doi:10.1186/1532-429X-14-88

22. Nakamori S, Dohi K, Ishida M, Goto Y, Imanaka-Yoshida K, Omori T, Goto I, Kumagai N, Fujimoto N, Ichikawa Y, Kitagawa K, Yamada N, Sakuma H, Ito M (2017) Native T1 Mapping and Extracellular Volume Mapping for the Assessment of Diffuse Myocardial Fibrosis in Dilated Cardiomyopathy. JACC Cardiovasc Imaging. doi:10.1016/j.jcmg.2017.04.006

23. Asleh R, Briasoulis A, Kremers WK, Adigun R, Boilson BA, Pereira NL, Edwards BS, Clavell AL, Schirger JA, Rodeheffer RJ, Frantz RP, Joyce LD, Maltais S, Stulak JM, Daly RC, Tilford J, Choi WG, Lerman A, Kushwaha SS (2018) Long-Term Sirolimus for Primary Immunosuppression in Heart Transplant Recipients. J Am Coll Cardiol 71 (6):636-650. doi:10.1016/j.jacc.2017.12.005

24. Eisen HJ, Tuzcu EM, Dorent R, Kobashigawa J, Mancini D, Valantine-von Kaeppler HA, Starling RC, Sorensen K, Hummel M, Lind JM, Abeywickrama KH, Bernhardt P, Group RBS (2003) Everolimus for the prevention of allograft rejection and vasculopathy in cardiac-transplant recipients. N Engl J Med 349 (9):847-858. doi:10.1056/NEJMoa022171

25. Clemmensen TS, Holm NR, Eiskjaer H, Jakobsen L, Berg K, Neghabat O, Logstrup BB, Christiansen EH, Dijkstra J, Terkelsen CJ, Maeng M, Poulsen SH (2018) Detection of early changes in the coronary artery microstructure after heart transplantation: A prospective optical coherence tomography study. J Heart Lung Transplant 37 (4):486-495. doi:10.1016/j.healun.2017.10.014

26. Yamani MH, Haji SA, Starling RC, Tuzcu EM, Ratliff NB, Cook DJ, Abdo A, Crowe T, Secic M, McCarthy P, Young JB (2002) Myocardial ischemic-fibrotic injury after human heart transplantation is associated with increased progression of vasculopathy, decreased cellular rejection and poor long-term outcome. J Am Coll Cardiol 39 (6):970-977

27. Armstrong AT, Binkley PF, Baker PB, Myerowitz PD, Leier CV (1998) Quantitative investigation of cardiomyocyte hypertrophy and myocardial fibrosis over 6 years after cardiac transplantation. J Am Coll Cardiol 32 (3):704-710

28. Cassar A, Matsuo Y, Herrmann J, Li J, Lennon RJ, Gulati R, Lerman LO, Kushwaha SS, Lerman A (2013) Coronary atherosclerosis with vulnerable plaque and complicated lesions in transplant recipients: new insight into cardiac allograft vasculopathy by optical coherence tomography. Eur Heart J 34 (33):2610-2617. doi:10.1093/eurheartj/eht236

29. Clemmensen TS, Holm NR, Eiskjaer H, Logstrup BB, Christiansen EH, Dijkstra J, Barkholt TO, Terkelsen CJ, Maeng M, Poulsen SH (2017) Layered Fibrotic Plaques Are the Predominant Component in Cardiac Allograft Vasculopathy: Systematic Findings and Risk Stratification by OCT. JACC Cardiovasc Imaging 10 (7):773-784. doi:10.1016/j.jcmg.2016.10.021

Authors' contributions

RBvH, JAMB, JY, and GG acquired, analysed and interpreted the CMR data. JFI and SD acquired, analysed and interpreted the OCT and X-ray data. SR and JLB performed and analysed the histology and interpreted its results. MK and PT performed the transplantation surgery. MK, JR, NL, and PT recruited subjects and collected clinical data. RBvH, MS, and RH designed the study and integrated the various results. RBvH and RH drafted the initial manuscript. All authors read and approved the final manuscript.

Figure captions

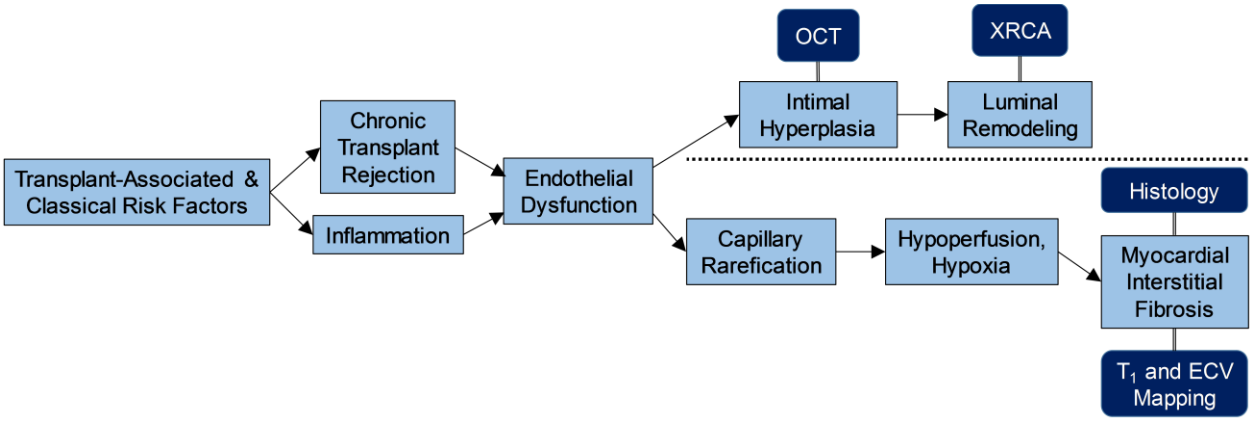

Figure 1. Simplified pathogenesis of CAV with positioning of each of the examinations. Note that the time scale on the upper and lower part of the right side of the diagram are not the same.

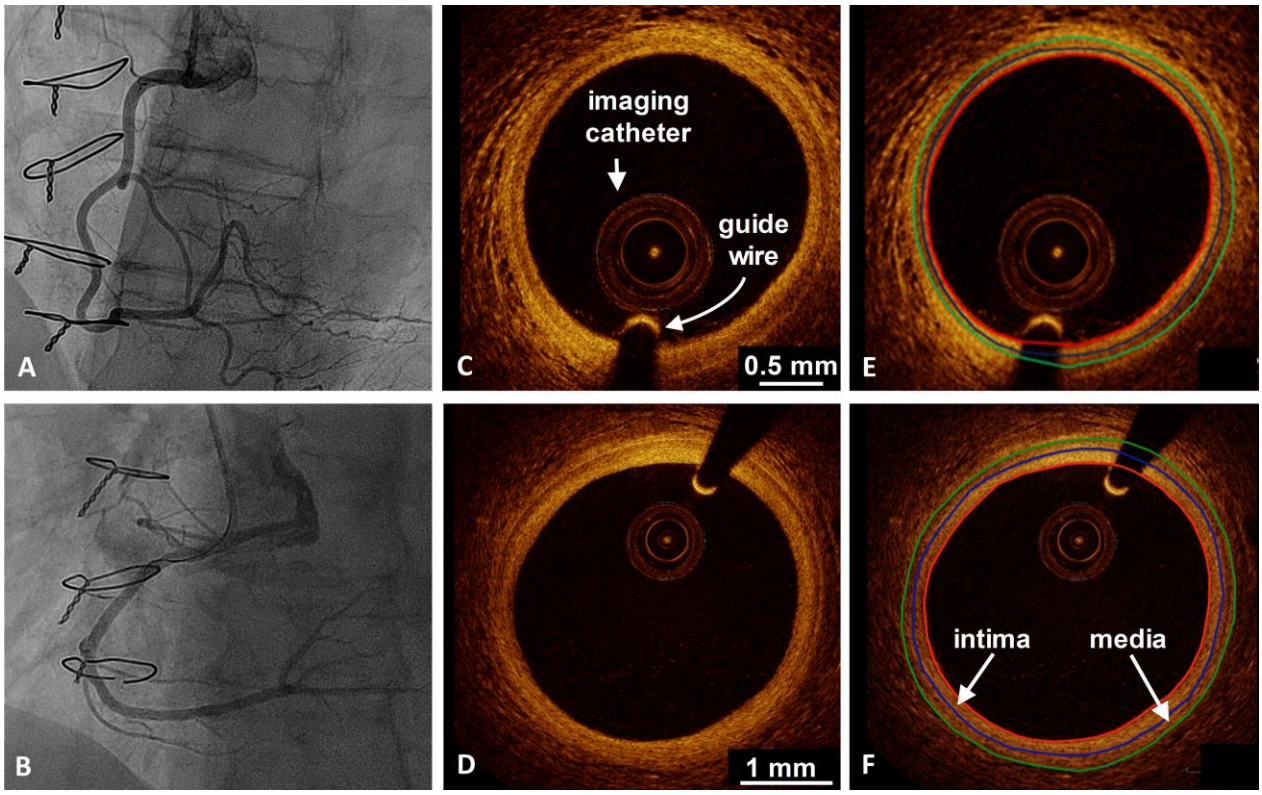

Figure 2. Established detection of CAV through its coronary sequelae. A) An XRCA of the right coronary artery (RCA) of a heart transplant recipient without CAV. Note the sternal wires from the transplantation surgery. **B)** A similar XRCA in a patient with CAV degree 1. Slight atheromatosis can be observed as an irregular border all along the RCA, but no significant lesions are visible. **C)** OCT image of the right coronary artery in the same patient without CAV. The tunica intima and media can be seen as the lighter inner and darker outer vessel wall, respectively. **D)** In the same patient with CAV, the tunica intima is visibly much thicker. **E-F)** Segmentations of the same OCT images. Red indicates the inside of the intima, blue the intima-media border, and green the media-adventitia border.

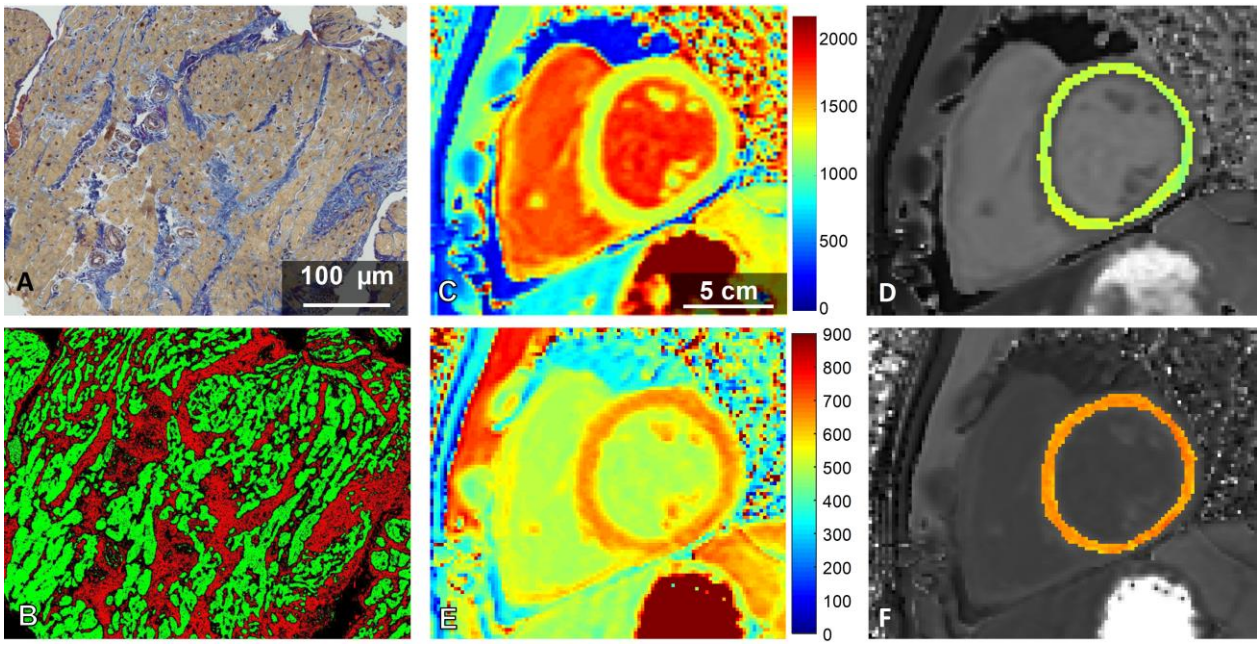

Figure 3. Quantification of myocardial interstitial fibrosis. A) An EMB is stained blue for collagen and brown for muscle. **B)** Automated segmentation of the same slide, with a clear delineation of myocytes (green) and fibrosis (red). **C)** A midventricular native T_1 map demonstrates a homogeneous myocardium with slightly elevated relaxation times (T_1=1232±46 ms). Scale bar in ms. **D)** The segmented myocardium in colour overlaid on the rest of the map. **E)** Post-contrast T_1 map at the same location. Note the different scale. **F)** Segmented myocardium of the post-contrast T_1 map. The ECV calculated from the two T_1 maps was 32.7±1.4%. Note that the ECV was not mapped pixel-wise, but was calculated from the averaged value of the entire segmented myocardium.

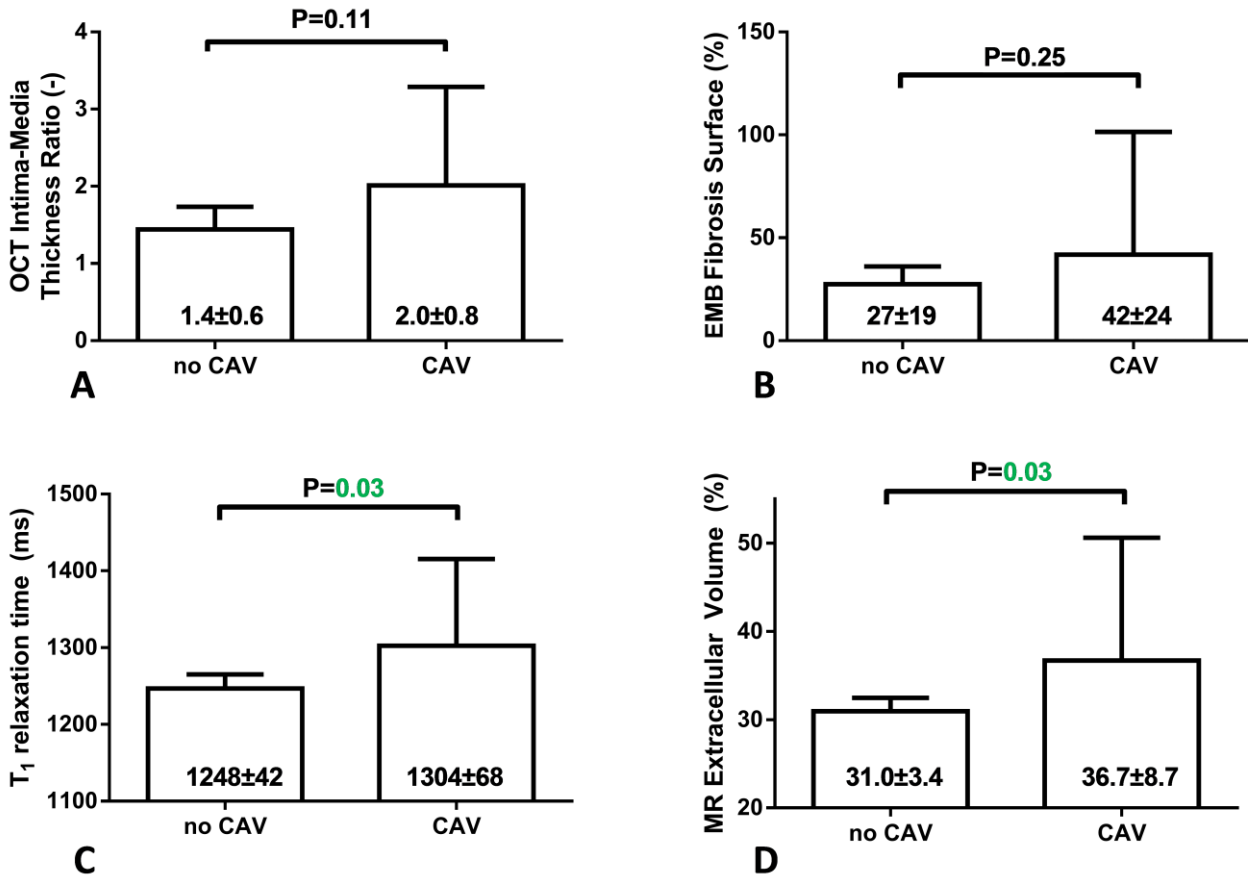

Figure 4. Effects of cardiac allograft vasculopathy (CAV) as observed on X-ray coronary angiography. A-B) The intima-media ratio obtained with OCT and the percentage of fibrosis in biopsies show a non-significant trend towards elevation in the presence of CAV as determined by XRCA. **C-D)** Patients with CAV demonstrated a significantly higher T_1 relaxation time and ECV than their counterparts without CAV. Numbers state the mean ± standard deviation; error bars indicate the 95% confidence interval.

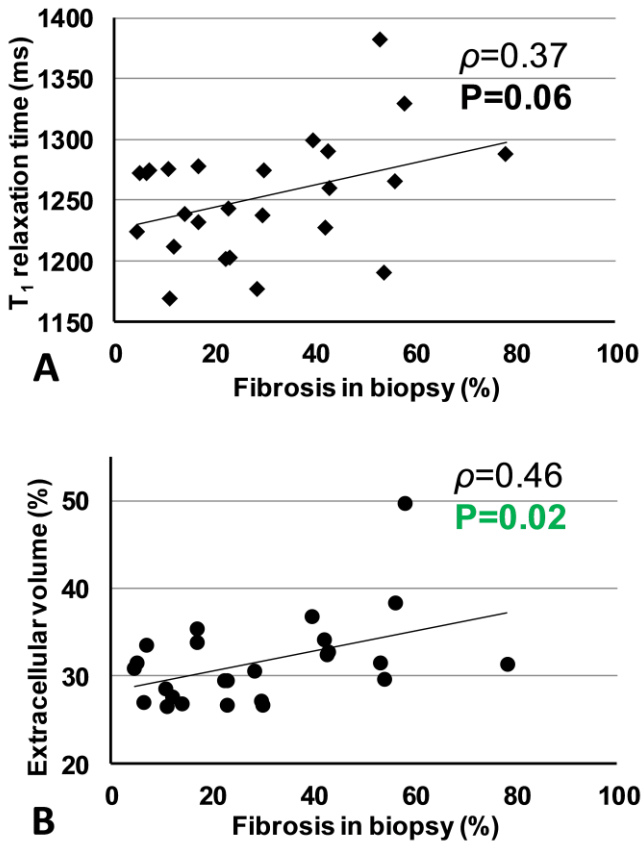

Figure 5. Correlations of biopsy-derived interstitial fibrosis and parametric mapping. The Pearson correlation coefficient ρ and its significance P are indicated. **A-B)** EMB fibrosis correlates weakly with the T_1 relaxation time and strongly with the ECV in the patient cohort.

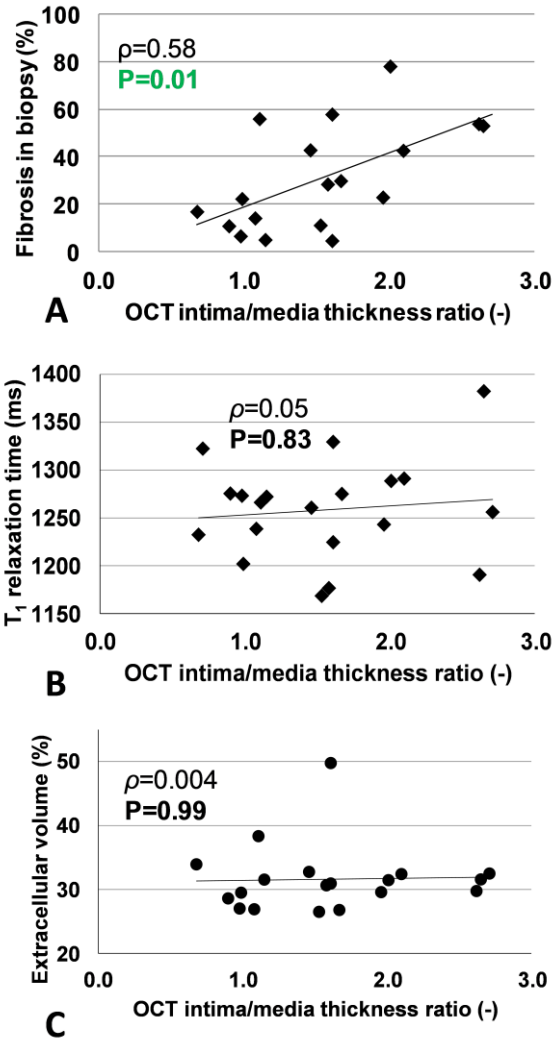

Figure 6. Correlation between the OCT intima-media thickness ratio (IMTR) and the measurements of interstitial fibrosis. A) Despite assessing the tentative effects of CAV at different locations in the heart, IMTR and the interstitial fibrosis in the EMB correlate significantly. **B-C)** There is no correlation between the IMTR and either myocardial T1 relaxation time or ECV.

Tables

Table 1. Baseline demographics of the recruited patient population.

Age (y)	54±13
Sex (female; % of patients)	30
Race (Caucasian; % of patients)	100
Time from transplant to OCT (y)	5.4±3.7
Indication for transplant	
Ischemic cardiomyopathy (% of patients)	30
Dilated non-ischemic cardiomyopathy (% of patients)	70
Donor age (y)	38.1±15.4
PRA>20 at transplant (% of patients)	0
CMV mismatch (% of patients)	52
Induction with basiliximab (% of patients)	63
>2 treated acute cellular rejections (% of patients)	22
Immunosuppression	
Cyclosporine (% of patients)	41
Tacrolimus (% of patients)	48
Myocphenolate mofetil (% of patients)	81
Everolimus (% of patients)	22
Diabetes (% of patients)	11
Aspirin use (% of patients)	37
Statin use (% of patients)	74
Total cholesterol (mmol/L)	4.4±1.3
LDL cholesterol (mmol/L)	2.2±1.0

Triglycerides (mmol/L)	2.1±1.7
Acute cellular rejection in the index EMB (%)	0

*OCT = optical coherence tomography, PRA = panel-reactive antibodies, CMV = cytomegalovirus, LDL = low-density lipoprotein, EMB = endomyocardial biopsy

Table 2. Summary of the main findings with the different modalities. Continuous variables are reported as mean ± standard deviation in all patients, followed by the range.

X-ray coronary angiography	
Procedure successful (% of all patients)	100 (27/27)
XRCA-CAV positive (% of procedures)	15 (4/27)
Non-significant focal atherosclerotic lesions (% of procedures)	41 (11/27)
Optical coherence tomography	
Procedure successful (% of all patients)	74 (20/27)
Presence of IMTR>1 (% of procedures)	75 (15/20)
IMTR (-)	1.56±0.63 (0.68-2.71)
Endomyocardial biopsy	
Procedure successful (% of all patients)	93 (25/27)
Degree of interstitial fibrosis (%)	29±20 (5-78)
Cardiac magnetic resonance	
Procedure successful (% of all patients)	100 (27/27)
Native T_1 relaxation time (ms)	1256±49 (1169-1382)
ECV (%)	31.9±4.8 (26.5-49.8)

XRCA = X-ray coronary angiography, CAV = cardiac allograft vasculopathy, IMTR = intima-media thickness ratio, ECV = extracellular volume